Research on Nonlinear Robust Control of Steering/Braking System of Heavy-duty Vehicle

Junning Zhang[1,(1)], Shaopu Yang[1,2,(2)], Yongjie Lu[1,2,(3)], Shaohua Li[1,2,(4)] Haoyang Fan[1]

1.School of Mechanical Engineering, Shijiazhuang Tiedao University; 2. State Key Laboratory of Mechanical Behavior in Traffic Engineering Structure and System Safety, Shijiazhuang City, Hebei Province, China

(1) zhangtinian@163.com,(2) yangsp@stdu.edu.cn,(3) luyongjie825@gmail.com,(4) lshsjz@163.com

Abstract - **There is a strong coupling relationship between vehicle steering and braking process, which affects vehicle driving safety and handling stability. A nonlinear robust control system is proposed in this paper. To improve the robustness and the coordination of the whole system, a nonlinear robust controller based on Hamilton function method is designed according to the nonlinear comprehensive model of the vehicle steering and braking. The dissipative Hamilton realization of this controller is obtained by a state pre-feedback technique. The stability and the validity of the control algorithm are validated by simulation results.**

I. INTRODUCTION

When a vehicle is driving on a complex linear road (multi-curved road, long slope, etc.), the road adhesion coefficient will change with time and abruptly due to the influence of the surrounding environment. The driver needs to adjust the safe driving speed from time to time, thus increasing the driver's driving fatigue and becoming a frequent area of traffic accidents. When a vehicle is driving on a road with abrupt or gradual change of road adhesion coefficient or linear change, if the driver is not aware of it in time and the speed of the vehicle fails to fall in time, slip or rollover or slip accompanied by rollover will occur, resulting in traffic accidents. Therefore, it is of great research value and application value to combine effective control strategies to achieve safe vehicle speed and ensure safe driving of vehicles.

Centrifugal force and longitudinal braking force are generated when vehicle steering and braking. These forces transfer the load of each tire, and then change the maximum longitudinal adhesion and lateral stiffness of each tire. The coupling relationship between steering angle and longitudinal braking force increases the complexity of tire cornering characteristics and the difficulty of steering braking safety and stability control. Therefore, the robust adaptive performance of automobile control system must be improved[6~10].

Vehicle system is a complex non-linear strong coupling system, which shows strong coupling interference and environmental interference between steering system and braking system. Traditional linear control is difficult to achieve satisfactory control effect. Hamilton function method can make full use of the inherent non-linear structural characteristics of the system in controller design. The structure of the controller is simple and easy to implement, and it has been well applied in the field of power system[11~14]. Based on the comprehensive model of vehicle steering and braking, a nonlinear robust coordinated controller is designed in this paper. Firstly, the Hamilton energy function of the system is constructed, and the nonlinear control strategy of steering and braking is designed according to the preset feedback. The simulation results verify the effectiveness of the designed control algorithm.

II. NONLINEAR COMPREHENSIVE MODEL OF HEAVY-DUTY VEHICLE

As shown in Fig.1 (the light-colored tire is the equivalent tire), the three degrees of freedom of the linear system are lateral motion, yaw motion and roll motion. In the figure, m is the

978-1-7281-3666-0/19/$31.00 ©2019 IEEE

vehicle mass; h'_θ is the distance from the spring-loaded mass center to the roll center; h_θ is the height of the spring-loaded mass center CG relative to the roll center RC; h_{RC} is the height from the roll center of the vehicle to the ground; l is the wheelbase of the left and right wheels; θ_x is the roll angle of the spring-loaded mass; F_{zl} and F_{zr} are the vertical loads of the left and right wheels; θ is the front wheel angle; r is the yaw rate, and β is the roll center of mass. α_f, α_m and α_r are the side slip angles of front, middle and rear wheels. a and f are the center of mass to front and middle axle wheelbase, and b is the distance from center to rear axle. v_x and v_y represent the longitudinal and lateral velocity of the center of mass, respectively. F_{yf}, F_{ym} and F_{yr} represent the total lateral forces of front, middle and rear wheels, respectively. a_y is the lateral acceleration at the center of mass.

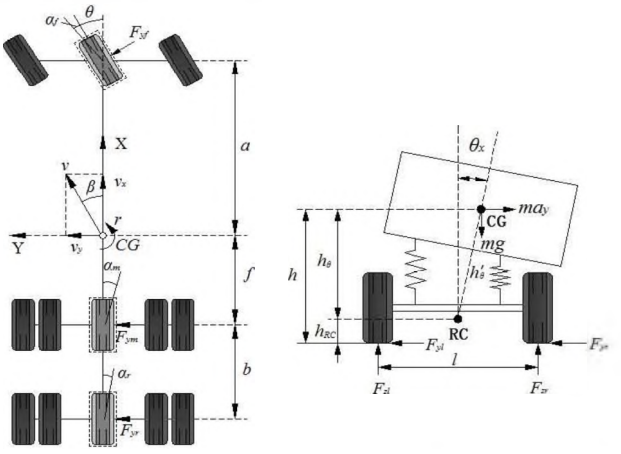

Fig. 1: Schematic Diagram of Dynamic Model of Three-axle Heavy-duty Vehicle

The main features of vehicle steering dynamics in a horizontal plane can be described by the single-track model. Considering the influence of the height of the CG, this model is extended by the vehicle's roll dynamics. For straight driving at constant speed the following linear differential equations represent the vehicle's lateral, yaw and roll dynamics:

$$m\left(\dot{v}_x - v_y r\right) = \left(F_{x\_fl} + F_{x\_fr}\right)\cos\theta + F_{x\_ml} + F_{x\_mr} + F_{x\_rl} + F_{x\_rr} + F_{y1}\sin\theta \quad (1)$$

$$mv_x\left(\dot{\beta} + r\right) = \left(C_v + 2C_h\right)\beta + \frac{C_v a - C_h f - C_h\left(f+b\right)}{v_x} - C_v\theta \quad (2)$$

$$I_z\dot{r} = \left(C_v a - C_h f - C_h\left(f+b\right)\right)\beta + \frac{\left(C_v a^2 + C_h f^2 + C_h\left(f+b\right)^2\right)}{v_x} r - aC_v\theta - M_z \quad (3)$$

In the formula, C_v is the front wheel sideslip characteristic parameter; C_h is the mid-rear wheel sideslip characteristic parameter; beta is the vehicle sideslip angle; I_Z is the moment of inertia of the vehicle around the center of mass; and M_Z is the vehicle yaw moment generated by the longitudinal braking force.

The linearization of the above dynamic equations can be reduced to equations (4), (5) and (6),

$$\dot{\beta} = \frac{C_v + 2C_h}{mv_x}\beta + \left(\frac{C_v a - C_h f - C_h\left(f+b\right)}{mv_x^2} - 1\right) r - \frac{C_v a}{I_z}\theta - \frac{M_z}{I_z} + \frac{M_n}{I_z} \quad (4)$$

$$\dot{r} = \frac{C_v a - C_h f - C_h\left(f+b\right)}{I_z}\beta + \frac{C_v a^2 + C_h f^2 + C_h\left(f+b\right)^2}{I_z v_x} r - \frac{C_v a}{I_z}\theta - \frac{M_z}{I_z} + \frac{M_n}{I_z} \quad (5)$$

$$\dot{v}_x = \beta r v_x - \frac{C_v}{m}\left(\beta + \frac{a}{v_x} r\right)\theta - \frac{\sum_{i,j} F_{x\_ij}}{m} + \frac{F}{m} \quad (6)$$

Where M_n, F is the disturbance force torque and the corresponding degree of freedom, reflects between the steering system and braking system coupling interference and the interference of environment.

In this paper, the dissipative Hamilton energy function method is applied to design the nonlinear stability controller.

State variables: $X = \left[x_1\ x_2\ x_3\right]^T = \left[\beta\ r\ v_x\right]^T$

Control input variables: $U = \left[u_1\ u_2\ u_3\right]^T = \left[\theta\ M_z\ \sum_{i,j} F_{x\_ij}\right]^T$

Disturbance variable: $W = \left[M_n\ f\right]^T$.

$$G_1(X)=\begin{bmatrix} -\frac{C_v}{mv_x} & 0 & 0 \\ -\frac{C_v a}{I_z} & -\frac{1}{I_z} & 0 \\ -\frac{C_v}{m}\left(\beta+\frac{a}{v_x}r\right) & 0 & -\frac{1}{m} \end{bmatrix}, \quad G_1(X)=\begin{bmatrix} 0 & 0 \\ \frac{1}{I_z} & 0 \\ 0 & \frac{1}{m} \end{bmatrix},$$

$$R(X)=\begin{bmatrix} 0 & 1 & 0 \\ 0 & 0 & 0 \\ 0 & 0 & 0 \end{bmatrix},$$

$$J(X)=\begin{bmatrix} \frac{C_v+2C_h}{mv_x} & \frac{C_v a-C_h f-C_h(f+b)}{mv_x^2} & 0 \\ \frac{C_v a-C_h f-C_h(f+b)}{I_z} & \frac{C_v a^2+C_h f^2+C_h(f+b)^2}{I_z v_x} & 0 \\ 0 & 0 & \beta r \end{bmatrix},$$

$h(X)=diag(\lambda_1,\lambda_2,\lambda_3)$, $\lambda_i>0(i=1,2,3)$.

Take Hamilton energy function as

$$H(X)=\frac{1}{2}\beta^2+\frac{1}{2}r^2+\frac{1}{2}v_x^2.$$

From the formula above, we can get

$$\nabla H(X)\triangleq\frac{\partial H}{\partial X}=[\beta\ r\ v_x]^T.$$

The final controller expression is as follows

$$\begin{aligned} \theta&=\left(\frac{1}{2}\lambda_1^2+\frac{1}{\gamma^2}\right)\left(\frac{C_v}{mv_x}\beta+\frac{C_v a}{I_z}r+\frac{C_v}{m}(\beta v_x+ar)\right) \\ M_z&=\left(\frac{1}{2}\lambda_1^2+\frac{1}{\gamma^2}\right)\frac{1}{I_z}r \\ \sum_{i,j}F_{x\_ij}&=\left(\frac{1}{2}\lambda_1^2+\frac{1}{\gamma^2}\right)\frac{1}{m}v_x \end{aligned} \tag{7}$$

III. SIMULATION ANALYSIS

The whole process of simulation is carried out in MATLAB/Simulink, and the simulation conditions are selected as double Line-Changing conditions. This paper set $h(X)=10I$, $\gamma=10$, and $c_0=\Delta=0.1$.

1. The control effect of different speeds

(1) The initial speed of the simulation is 46 km/h and the height of the center of mass is 1.0 m. The angular displacement curve of the front wheel steering is shown in Fig. 2. Fig. 3 shows the dynamic lateral load transfer rate LTR', when the vehicle is steering and braking. It can be seen from the figure that the vehicle is in danger of rollover at 5.413 s and 10.76 s. The amplitude of roll angle displacement (as shown in Fig. 4) and yaw rate(as shown in Fig. 5) are significantly less than those without control. In theory, this control can improve the steering stability of vehicles.

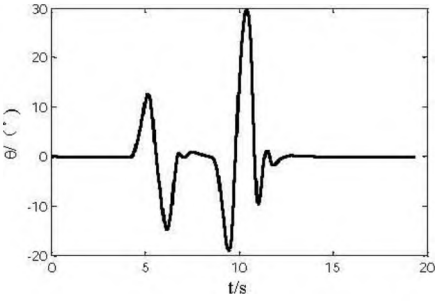

Fig.2: Front wheel steering angle(input)

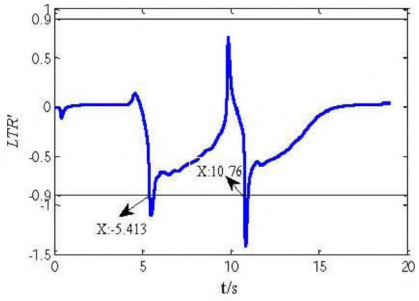

Fig.3: Dynamic lateral load transfer ratios

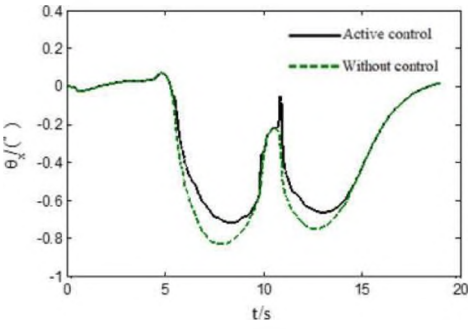

Fig.4: Side-slip angle of vehicle center of mass

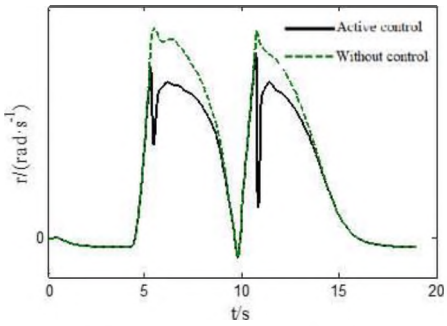

Fig.5 Yaw-rate of vehicle center of mass

(2) The initial speed of the simulation is 35 km/h and the height of the center of mass is 1.0 m. The angular displacement curve of the front wheel steering is shown in Fig. 6. Fig. 7 shows the dynamic lateral load transfer rate LTR', when the vehicle is steering and braking. The absolute value of dynamic lateral load transfer rate LTR' is less than 0.5 when vehicle steering and braking, so there is no trend of rollover when vehicle completes the whole steering process. Vehicle roll angle displacement amplitude (as shown in Figure 8) and yaw rate amplitude (as shown in Figure 9) can be seen that there are no obvious braking signs when steering, can be roughly regarded as no braking.

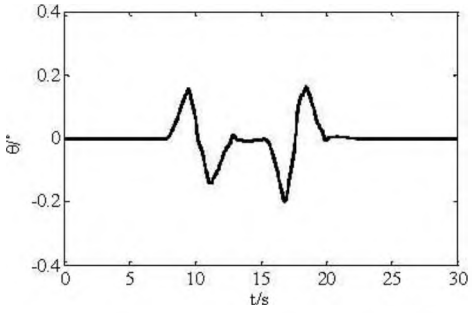

Fig.6: Front wheel steering angle(input)

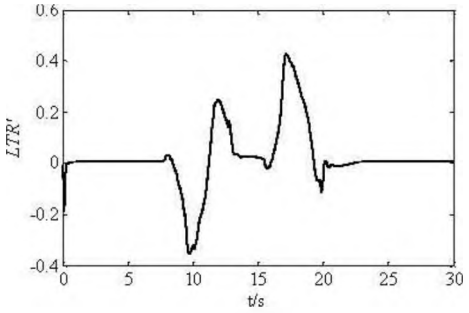

Fig.7: Dynamic lateral load transfer ratios

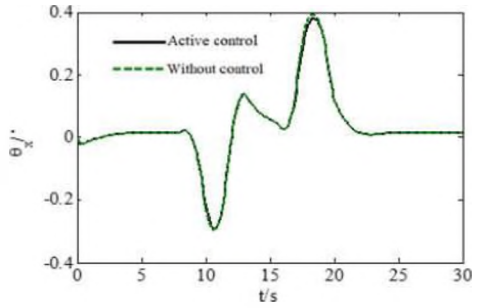

Fig.8: Side-slip angle of vehicle center of mass

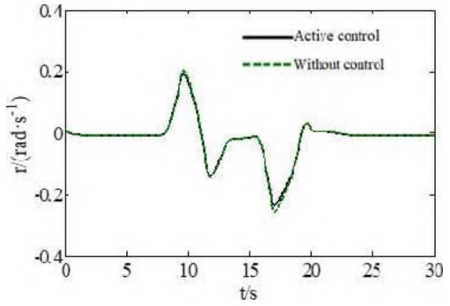

Fig.9: Yaw-rate of vehicle center of mass

2. The control effect of different centroid heights

When the loads of heavy-duty vehicle are different, the height of body mass center will be affected. It is necessary to compare and analyze the control effect of rollover under different body height.

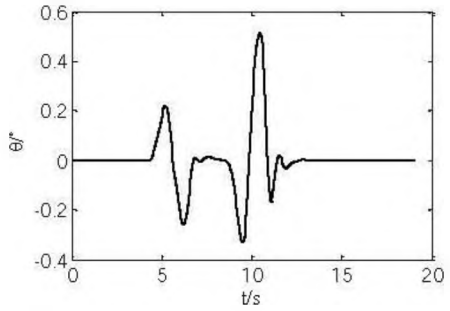

Fig.10: Front wheel steering angle(input)

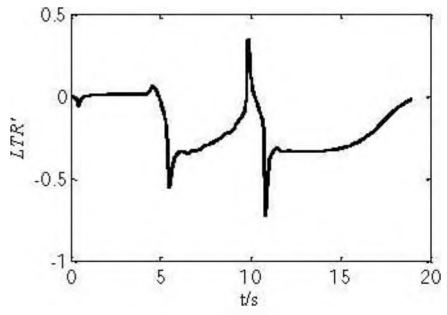

Fig.11: Dynamic lateral load transfer ratios

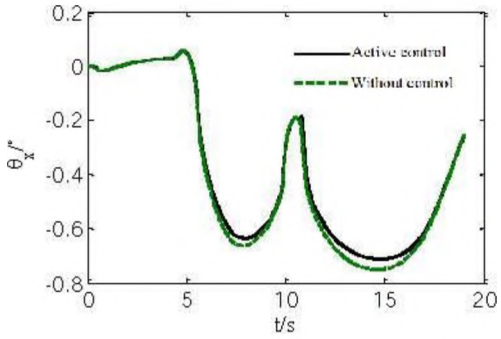

Fig.12: Side-slip angle of vehicle center of mass

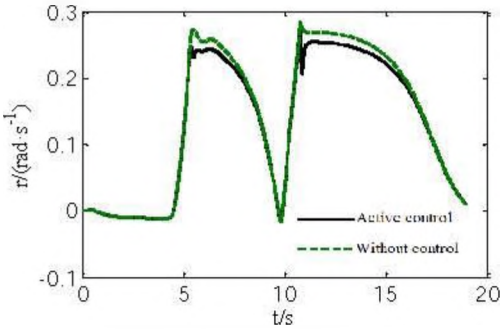

Fig.13: Yaw-rate of vehicle center of mass

(1) The initial speed of the simulation is 46 km/h and the height of the center of mass is 0.8 m. The angular displacement curve of the front wheel steering is shown in Fig. 10. Fig. 11 shows that the absolute value of dynamic lateral load transfer rate LTR' is less than 0.9 during steering and braking, so there is no risk of rollover during the whole steering process. Vehicle roll angular displacement amplitude (shown in Figure 12) and yaw rate amplitude (shown in Figure 13) are reduced compared with uncontrolled vehicles. In theory, this control can reduce the possibility of rollover during vehicle steering.

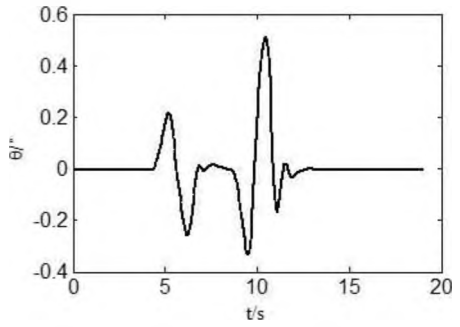

Fig.14: Front wheel steering angle(input)

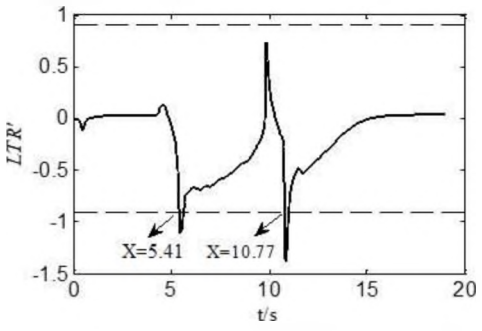

Fig.15 Dynamic lateral load transfer ratios

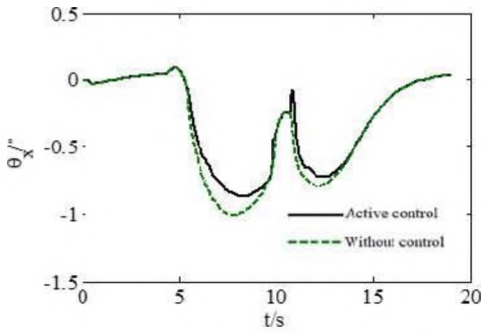

Fig.16: Side-slip angle of vehicle center of mass

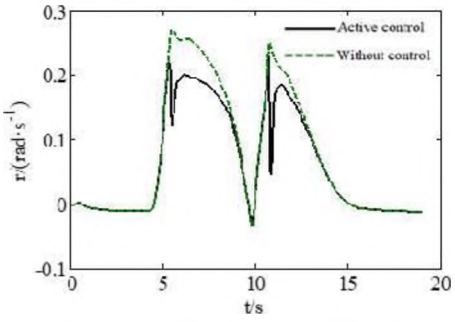

Fig.17 Yaw-rate of vehicle center of mass

(2) The initial speed of the simulation is 46 km/h and the height of the center of mass is 1.2 m. The angular displacement curve of the front wheel steering is shown in Fig. 14. Fig. 15 shows the dynamic lateral load transfer rate LTR', and the risk

of rollover when the vehicle is steering and braking in 5.41 s and 10.77 s. The amplitude of roll angle displacement (as shown in Fig. 16) and yaw rate (as shown in Fig. 17) are significantly less than those without control. In theory, this control method can reduce the possibility of rollover when the vehicle is steering.

IV. CONCLUSION

(1) A three-degree-of-freedom non-tripping rollover dynamic model of Heavy-duty vehicles is established, and the simulation analysis of non-tripping rollover warning of Heavy-duty vehicles is carried out. An improved TTR (Time-To-Rollover) rollover early warning algorithm based on the estimation of rollover angle of Heavy-haul vehicle body is designed by using LTR (Lateral-load Transfer Rate) as the threshold index of rollover early warning. It realizes the prediction of the rollover time of heavy-duty vehicles in the future.

(2) The control effect of vehicle steering is analyzed from two aspects of vehicle speed and centroid height. The simulation results show that the rollover of heavy-duty vehicles may occur in a short time due to the high centroid or too fast speed, which can be controlled by steering/braking control, thus avoiding the rollover of heavy-duty vehicles to the greatest extent. In theory, the control can improve the steering stability of vehicles.

V. ACKNOWLEDGMENTS

The Central Guide to Local Science and Technology Development Project(18242219G), National Natural Science Foundation of China (11572207,11872255,11472180), Natural Science Foundation of Hebei Province (Grant No. A2016210103) and Hebei Education Department(Grant No. CXZZBS2018145).

VI. REFERENCES

[1] Esmailzadeh E, Goodarzi A, Vossoughi G R. Optimal yaw moment control law for improved vehicle handling[J]. Mechatron-ics, 2003, 13(7): 659-675.

[2] Odenthal D, Bunte T, Ackermann J. Nonlinear steering and braking control for vehicle rollover avoidance[C]// Control Conference. 2015.

[3] Chen W W, Chu C B. Electric power steering system and anti-lock braking system based on layered coordinated control[J].Journal of Mechanical Engineering, 2009, 45(7): 188-193.

[4] Jo, J. S, You, et al. Vehicle stability control system for enhancing steerabilty, lateral stability, and roll stability[J]. International Journal of Automotive Technology, 2008, 9(5):571.

[5] Li J W, Zhang G G, Wang Y H. Study on Vehicle Stability Based on Coordinated Control of Direct Yaw Moment Control and Slip Rate Control[J]. Applied Mechanics & Materials, 2012, 220-223:597-600.

[6] Yu J S. A robust adaptive wheel-slip controller for antilock brake system[C]// IEEE Conference on Decision & Control. 1997.

[7] Liang C, Liang Y, Zhao Z, et al. Study of a Method for Improving the Anti-lock Brake System of Electric Vehicle[J]. Applied Mechanics & Materials, 2012, 157-158:542-545.

[8] Yazdanpanah R, Mirsalim M. Design of robust speed and slip controllers for a hybrid electromagnetic brake system[J]. Iet Electric Power Applications, 2015, 9(4):307-318.

[9] Lin Z, Luo Y, Jing K, et al. Anti-lock Braking System's Performance of Vehicle Using Hardware in-the-Loop Techniques[C]// Sixth International Conference on Intelligent Systems Design & Engineering Applications. 2015.

[10] Bera T K, Bhattacharya K, Samantaray A K. Evaluation of antilock braking system with an integrated model of full vehicle system dynamics[J]. Simulation Modelling Practice & Theory, 2011, 19(10):2131-2150.

[11] Zhang X, Zhao K, Sun L. A PMSM sliding mode control system based on a novel reaching law[J]. Proceedings of the Csee, 2011, 31(24):1-5.

[12] Zhang Y F, Li S J, Zhou Y, et al. PMSM Control System Based on a Improved Sliding Mode Observer[J]. Applied Mechanics & Materials, 2013, 307:27-30.

[13] Su Y X, Zheng C H, Duan B Y. Automatic disturbances rejection controller for precise motion control of permanent-magnet synchronous motors[J]. IEEE Transactions on Industrial Electronics, 2005, 52(3):814-823.

[14] Siraramírez H, Linaresflores J, Contrerasordaz M A. On the Control of the Permanent Magnet Synchronous Motor: An Active Disturbance Rejection Control Approach[J]. IEEE Transactions on Control Systems Technology, 2014, 22(5):2056-2063.